

DUPLICATE ALSO

Met.O.19 BRANCH MEMORANDUM No. 100

Bias Elimination and Scatter in Lightning Location by the  
VLF Arrival Time Difference Technique

by

A. C. L. Lee

November 1989

Met O 19b,  
Meteorological Office, Bracknell,  
Berkshire, RG12 2SZ, United Kingdom

LONDON, METEOROLOGICAL OFFICE.  
Met.O.19 Branch Memorandum No.100

Bias elimination and scatter in lightning  
location by the VLF arrival time difference  
technique.

10061189

551.501.83  
551.594.221  
681.2.08

FH5B

Note: This paper has not been published. Permission to quote from it should be obtained from  
(Engineering Instrumentation), Meteorological Office, Building Y70,  
D.

ARCHIVE Y42.J2

National Meteorological Library  
and Archive

Archive copy - reference only



## ABSTRACT

In the very low frequency (VLF) band lightning flashes are detectable at ranges of several thousand kilometres. Studies of experimental data show that if systematic biases were eliminated from the United Kingdom Meteorological Office's VLF arrival time difference (ATD) flash locating (fixing) system, the residual ATD scatter would amount to 1.4–2  $\mu$ s. For the operational outstation network this would give flash fixing errors below 1.2 km over most of western Europe. Techniques are presented for the elimination of bias to approach this precision. At longer ranges propagation effects, including those due to terrain conductivity, must be considered.

## 1 Introduction

A number of network systems now exist for the remote location of lightning flashes with useful accuracy over ranges of hundreds or thousands of kilometres. One of the earliest systems put into operational use, and only recently retired, was the Cathode-Ray Direction Finding (CRDF) System (Ockenden, 1947; Maidens, 1953) which used crossed-loop antennae at a number of outstations to measure the apparent bearing of lightning-induced radio atmospherics ('sferics') within a narrow bandwidth centred on a frequency of approximately 10 kHz. In this very low frequency (VLF) band, energy emitted from a lightning stroke — particularly energy emitted at a low angle of elevation from a nearly vertical return stroke (Lee, 1986a) — is strongly reflected (with some dispersion) off the ionospheric D-Layer, and then off the earth's surface (particularly a conducting sea-water surface). This earth-ionosphere waveguide ensures that return-strokes can be detected at VLF over ranges of thousands of kilometres and the lightning source located by triangulation. Unfortunately, crossed-loop direction finders suffer from various polarisation errors (caused by non-vertical source, propagation effects, and site effects; Horner, 1954) which degrade bearing measurements and thus location (or 'fix') accuracy. Propagation errors can amount to 1–2° of bearing by day, and 10° by night; and site errors can be much larger — although they are relatively static and can be largely calibrated out.

More recently, operational systems have been developed which reduce polarisation errors.

Herrman et al (1976) and Krider et al (1976) describe a gated wideband (1 kHz to 1 MHz) crossed-loop 'Magnetic Direction Finding' (MDF) development of the CRDF principle. MDF outstations use only the first 1–5  $\mu$ s of a return-stroke sferic's ground-wave, originating from the lowest portion of the discharge channel, a region that is usually nearly vertical. This reduces source polarisation, and discriminates against the later-arriving sky-waves which introduce propagation errors, although other forms of polarisation and site error remain (Lee, 1986a). The ground-wave's high frequencies, necessary for time discrimination, are unacceptably attenuated by the radio horizon beyond about 400 km, limiting range. However, bearing scatter (once bias has been removed) is reduced to around 1–2°. Fix error depends on bearing scatter through the network geometry, and also on the precision of site error calibration. The bearing scatter suggests a relative location error of around 7–30 km for flashes near the limits of range under favourable network geometries. MacGorman and Rust (1988) compared MDF fixes with optical fixes using video cameras, and obtained distributions of separation in location that peaked within 0–10 km at short ranges, and within 20–30 km at MDF ranges of 250 km — although a significant proportion of data exhibited much larger separations. This system is now well established over a large fraction of the USA, linked via a communication network, and provides rapid response information on lightning location and a detailed archive.

Lyons et al (1985) describe a 'Time of Arrival' (TOA) network system which avoids polarisation errors by timing sferic features rather than measuring bearings. Bent and Lyons (1984) describe how its wideband (2–500 kHz) electric field receivers identify and time the arrival of the initial peak within the first 1–5  $\mu$ s of a ground-wave (and therefore relatively distortion-free) return-stroke sferic. This short-duration peak can in principle be timed to 2  $\mu$ s or better against a Loran-C receiver standard, yielding flash location by a hyperbolic method, but only to ranges comparable with (perhaps somewhat greater than) the MDF system because of the high frequencies necessary for time discrimination. Location accuracy depends on network geometry. The TOA technique requires (at least) one more outstation to fix a flash than the MDF technique, so for equal reception range a TOA system requires a higher density of outstations than an MDF system. In principle location error can be low: under 1 km error



within a 200 km square formed by four outstations; but degrading rapidly with range to (say) 6 km at 400 km because baselines are necessarily short. MacGorman and Rust (1988) suggest distributions of separation between TOA and video fixes peaking between 10–20 km at short TOA ranges, and 0–10 km (*sic*) at 250 km TOA range. However, nearly a third of their data fall within separations between 40–140 km in a substantial distribution tail, suggesting the fixes are unreliable. This degradation against theoretical performance appears to be due to detailed limitations of the current hardware and software design. The TOA system is being modified to accept only self-consistent results derived from enough outstations to ensure an over-determined fix, which can indicate error and so improve quality control; although the necessary extra outstation(s) imply reduced network range or increased network density.

Scott's (1988) crossed-loop direction-finding system, using three United Kingdom (UK) outstations on a 250–350 km baseline, has resisted the trend towards higher frequencies, using extremely low frequencies (ELF) at 1 kHz. Detection efficiencies of 96% or higher at 400 km range are claimed. Yamashita and Sao's (1974a, b) propagation model (based on a simplified ionospheric structure) suggests that such a system should exhibit no source (and only small propagation) polarisation effects. However Cantor's (1967) measurements of substantial ELF sferics polarisation conflict with this simple theory, so polarisation errors may depend on ionospheric structure. Scott provides little quantified evidence of location error, but indicates from a combination of bearing inconsistency and comparison with (undisclosed) observer evidence a fix error of 4–7 km within an unspecified portion of the UK service area. Bearing scatter is not discussed, but the suggested size of fixed bearing errors is 0.5–1.5°.

Lee's (1986a) VLF arrival time difference (ATD) technique, the subject of this paper, has been installed as an operational network replacing the CRDF system (Lee, 1986b); and formally commenced automatic international product issue on 17 June 1988. Like the TOA system, the ATD system avoids polarisation errors associated with direction-finding by measuring (for each flash) differences between sferic arrival times at outstations. However it also avoids timing specific features on each sferic waveform, obtaining ATD through correlation between (smooth) VLF sferic waveforms received at different outstations; and so with no need for higher frequencies can detect sferics at ranges of many thousands of kilometres through the VLF earth-ionosphere waveguide. Thus few outstations are needed to cover a several-thousand kilometre diameter service area, and most outstations contribute to each fix. This latter effect implies that fix over-determination is easily achieved, giving a statistical reduction in fixing error; and ensures that a (self-consistency) measure of fix error is always available for quality control.

In this paper the ATD technique's limiting precision is quantified using experimental trial network data, and also data from the operational ATD network; although the non-operational algorithms used mean that the results may not be directly applied to the current operational system.

The ATD technique implements a passive coherent radar, and at typically high signal to noise ratios (SNRs) its ATD scatter is a small fraction of a VLF cycle, of order 1–3  $\mu$ s as demonstrated below. Fix errors with a scatter (after any bias removal) of hundreds of metres to a few kilometres are implied for ranges of a few hundred to a few thousand kilometres using a network of only seven (or fewer) outstations. The corresponding spatial error vectors subtend angles of only a few hundredths of a degree at the observing outstations, substantially smaller than bearing errors for other systems described above.

## 2 The 'size' of a distant lightning flash VLF image

Flash fixing to errors of only a few hundred metres (after bias removal) appears inconsistent with lightning structures where channels can extend over horizontal distances of many kilometres (Proctor, 1983). Lee (1989a) discusses this in detail for VLF observation; a brief summary is presented here.

VLF (and ELF) lightning sources are dominated by horizontally self-contained return strokes and K-processes rather than the extended stepped-leader structures observed at very high frequency; VLF earth-ionosphere waveguide propagation enhances radiation from vertically polarised sources, while attenuating radiation from horizontally polarised sources through phase reversal at the ground-mirror image source. Return-stroke electric current models show that VLF emission is mainly from the structure's lowest 1.5–3 km, of which the most heavily radiating lowest few hundred metres is often nearly vertical. Thus most VLF emission is from a region of under 1 km horizontal extent, close to the ground contact point.

At 9.766 kHz (the VLF centre frequency for the ATD system) the radiation wavelength is 31 km.



The 1 km horizontal extent of the VLF source is much less than a half-wavelength, so the radiation source is averaged into a well-defined 'centre of mass' whose position remains essentially independent (to within 10–30 m; Lee, 1989a) of the observation azimuth, allowing highly self-consistent measurements to be made. Systems using frequencies around 1 MHz (wavelength 300 m) suffer differential interference between source sub-structures separated horizontally by 150 m or so, creating target 'glint' where the observed source position varies between outstations, degrading fix errors.

### 3 The ATD sferics system

Fig. 1 is a simplified representation of the operational ATD system (Lee, 1986b). Each unmanned outstation senses the vertical electric field with a rod antenna and processes the analogue signal to produce a filtered analogue output with 2–18 kHz bandwidth, and digital 'event' signals when sferic-like waveforms exceed a threshold. The analogue signal is digitised and stored in a circular buffer within the Timing/Formatting unit, which contains a counter driven by a precision oscillator (normally a rubidium atomic oscillator) to establish a local timescale. When a sferic is detected, the event signal triggers the Timing/Formatting unit to send epoch and waveform data to the microprocessor to be stored, ensuring that 13.1  $\mu$ s of contiguous data always surrounds the event epoch. Each outstation is linked via a low-speed duplex communication channel to the control station, to which it may transmit this data.

The outstations normally operate independently, maximising sensitivity for limited outstation throughput by adapting their own thresholds; but one (the 'selector' outstation) has its threshold set artificially high by the control station (and thus is biased towards strong sferics, normally stored at most of the other outstations) to match the rate of data flow to control station resources. This selector passes the epoch values of its stored sferics to the control station, which then requests waveform and epoch ('flash') data from all outstations near these selected epochs.

The outstations send this data in compressed form to the control station — reducing the system 3 dB bandwidth to 8.1–11.7 kHz in the process.

For each flash, the control station chooses one of the associated outstation waveforms as a reference, and correlates each of the remaining  $r$  outstations' sferic waveform for that flash against this reference. The main correlation peak position gives the (measured)  $ATD_M(r)$ , while the amplitudes of the main and subsidiary peaks give SNRs from which estimates of ATD variance  $\sigma^2(r)$  can be inferred (Lee, 1986a).

The flash fix (latitude  $\phi$ , longitude  $\lambda$ ) may be deduced by minimising, with respect to  $\phi$ ,  $\lambda$ , the  $RESIDUAL^2(\phi, \lambda)$  obtained by weighting the squared differences between  $ATD_M(r)$  and the corresponding theoretical  $ATD_{TH}(r, \phi, \lambda)$ ; the latter based on the assumed fix, a spheroidal earth, and a modelled sferic phase velocity (Lee, 1986a), where:

$$RESIDUAL^2(\phi, \lambda) = \frac{1}{(m-2)} \sum_{r=1}^m \left\{ \frac{ATD_{TH}(r, \phi, \lambda) - ATD_M(r)}{\sigma(r)} \right\}^2 \quad (1)$$

and:

$m$  = No. of non-reference outstations (No. of ATD values).

$r$  = Index of non-reference outstations.

$ATD_{TH}$  = Theoretical ATD value.

$ATD_M$  = Measured ATD value.

$\phi$  = estimated flash latitude.

$\lambda$  = estimated flash longitude.

$\sigma(r)$  = ATD standard deviation for non-reference outstation.

The normalising factor  $(m-2)$  accounts for the number of degrees of freedom (DOF) involved in fixing, so that with correct  $\sigma(r)$  values the expectation for the minimum value of  $RESIDUAL$  is unity. Thus, if we assume a relation between the components of  $\sigma(r)$  (eg. they are equal) and average minimised  $RESIDUAL^2$  over many flashes; then re-scaling absolute  $\sigma^2(r)$  to give the expected mean  $RESIDUAL^2$  yields the best estimate ATD variance.

Finally, fixes are composited into messages for external distribution. The SFLOC coded message has been transmitted routinely over World Meteorological Organisation (WMO) channels for many years (based on CRDF products) but has a temporal resolution of 30 minutes and a spatial resolution



of  $0.5^\circ$ . A message with a resolution of 5 minutes and  $0.025^\circ$   $0.05^\circ$  is passed to the Synoptic Data Base on the Meteorological Office computer system for internal use, and the generation of guidance for specific customers. Data on individual flashes with much greater resolution are available to the control station operator, and can be printed.

The above processing details are automatically monitored for symptoms of problems, and continuously corrected. This includes automatic (or control-station operator directed) calibration of analogue filters, removal of interfering transmissions, reception and use of Loran-C, Omega, and other time-standard signals for accurate conversion of local epoch values to International Atomic Time, and multiplicity of many items to ensure robust performance.

The formal ATD system service area is  $40^\circ\text{W}$ – $40^\circ\text{E}$   $30^\circ$ – $70^\circ\text{N}$ , which exceeds the combined areas of the USA and Canada, although flashes can be usefully located well outside this area. Fig. 2 shows most of the service area, and the medium-term locations of the seven operational outstations at Lerwick (Shetlands), Stornoway (Scotland), Aughton (near Liverpool), Hemsby (East Anglia), Camborne (Cornwall), Gibraltar and Cyprus. These locations are pragmatic rather than ideal. Initially the Aughton station is being operated at Beaufort Park ( $51.4^\circ\text{N}$ ,  $0.8^\circ\text{W}$ ) with the control station to aid development. Fig. 2 shows contours of root mean square (RMS) fix error (km) for the outstations shown, in quarter-decade steps assuming  $5\ \mu\text{s}$  RMS ATD error. In practice, even smaller ATD errors are achievable (particularly for relative timing accuracy, indicating fix scatter) as discussed below, giving proportionally reduced fixing errors.

## 4 Estimation of absolute errors and scatter in ATD flash location

### a. Trials data - absolute fix errors

Lee (1986a) describes trials of the ATD concept using four low-cost outstations deployed over the UK at Beaufort Park, Camborne, and Shanwell ( $56.4^\circ\text{N}$ ,  $2.9^\circ\text{W}$ ), and at Gibraltar; and scales  $RESIDUAL^2$  to estimate ATD variance  $\sigma^2(r)$ . This estimate is strictly correct only if the errors are random - ie. there is no bias in the differences between theoretical and measured ATD values. Systematic effects such as timescale or propagation errors will add to the value, causing it to be a pessimistic estimate of the ultimate potential of the ATD technique. If bias errors are unknown, they can be modelled as random so that the estimate given can be interpreted as correct for all types of error; with the proviso that bias errors could eventually be reduced, and the remaining purely random errors regarded as scatter about a biased location.

The trial results demonstrated (total) ATD  $\sigma(r)$  errors of  $3.33$ – $10.9\ \mu\text{s}$ , with the larger errors almost certainly due to clock jump problems in the rudimentary trial equipment (Lee, 1986a). The more representative lower value is smaller than the  $5\ \mu\text{s}$  used in Fig. 2, corresponding to proportionally smaller (absolute) fix errors for the operational geometry, provided that all outstations contribute with this error to a fix.

### b. Indications of low levels of fixing scatter

Trial fixes tended to cluster into tight groups, presumably because of meteorological events, so the spread of grouped fixes indicates the spatial variance of the physical event, plus the fixing variance. When a group occurs over a small area and duration, then bias effects are probably constant, and the spread of the tightest of such groups gives an indication of fixing scatter. Unfortunately, trial outstations were synchronised through low selection-rate CRDF mechanisms, so the number of fixes within any group (which typically occurs over a storm cell lifetime) is small. Lee (1986a) lists several such groups with diameters  $1.7$ – $10.7\ \text{km}$  (the larger diameters corresponding to longer durations) observed in the Mediterranean area, at  $1000$ – $2000\ \text{km}$  outstation ranges.

Lee (1989b) discusses a trial case involving a tight group of intense sferics that appeared to be associated with an organised storm near  $45^\circ\text{N}$   $3^\circ\text{E}$  on the Massif Centrale in France. ATD variance over several flashes indicated an absolute fix error of around  $5\ \text{km}$ . The RMS spatial scatter of this group was  $1.06\ \text{km}$ , but it appeared to travel consistently with the local winds. If a uniform velocity fitted to this data is subtracted, the best estimate RMS Lagrangian spatial scatter (taking correct account of lost DOF) is reduced to  $0.5$ – $0.6\ \text{km}$ . However, as this group contained only  $3$ – $5$  flashes, all that can



be said with reasonable (90%) confidence is that on this occasion the fix scatter was representative of a population scatter that fell within 2.5 km RMS.

The spatial scatter of tightly grouped fixes can thus be smaller than the absolute fix error indicated by ATD variance, suggesting significant bias in the measurement. Bias removal would allow the underlying scatter, and hence the ultimate fixing precision, to be estimated.

### c. Estimation of Relative errors

Eqn (1) is suitable for estimating ATD variance from many flashes only when the same reference station can be used for all flashes. To accommodate different numbers of outstations (and different reference outstation) per flash, and systematic offsets  $O(r)$  for each outstation, it is convenient to re-cast (1) into a more explicit  $\chi^2$  form:

Consider flash  $s$  (of  $S$  flashes) whose sferics are received at  $R(s)$  outstations, indexed by  $r$ , within a network of  $R_{MAX}$  outstations. For the moment, consider an identifiable feature on each flash's sferics with arrival time  $T_M(s, r)$  measured at each of the respective outstations, and an emission time origin  $T_0(s)$ . Through an iterative process we may estimate the fix  $(\phi(s), \lambda(s))$ , and thus the theoretical sferic transit time from  $(\phi(s), \lambda(s))$  to outstation  $r$  as  $T_{TH}(r, \phi(s), \lambda(s))$ , using the models described for (1). The measured transit time (including errors) is  $(T_M(s, r) - T_0(s))$ , so we estimate fixes by minimising  $\chi^2$  with respect to all the flash positions, where:

$$\chi^2(\phi(1), \lambda(1), \dots, \phi(S), \lambda(S)) = \sum_{s=1}^S \sum_{r=1}^{R(s)} \left\{ \frac{\Delta T(s, r) - O(r)}{\sigma^*(r)} \right\}^2 \quad (2)$$

$$\Delta T(s, r) = (T_M(s, r) - T_0(s)) - T_{TH}(r, \phi(s), \lambda(s)) \quad (3)$$

and:

$S$  = Total number of flashes.

$s$  = Index to  $S$ .

$R(s)$  = No of outstations receiving sferics for flash  $s$ .

$O(r)$  = Estimate of offset introduced into outstation  $r$  timing (initially considered to be zero)

$T_0(s)$  = emission time of observable 'feature' on flash  $s$  waveform.

$T_M(s, r)$  = measured arrival time of flash  $s$  feature at outstation  $r$ .

$T_{TH}(r, \phi(s), \lambda(s))$  = Theoretical sferic transit time from assumed flash  $s$  location  $(\phi(s), \lambda(s))$  to outstation  $r$ .

$\sigma^*(r)$  = timing standard deviation for sferics received at outstation  $r$ .

other quantities as defined earlier, but on a by-flash basis.

The above description implies that  $T_M$  and  $T_0$  are measured on an absolute timescale, but as they are differenced we can initialise timescales for flash  $s$  at  $T_M(s, ref(s))$ , making  $T_M$  identical to the ATD value, with  $T_M = 0$  for the reference outstation  $ref(s)$ . Thus (2) and (3) are expressed in ATD terms, and we can drop references to identifiable features and use correlation techniques as before.

Minimisation of  $\chi^2$  with respect to unknown variables  $\phi(s)$ ,  $\lambda(s)$  and  $T_0(s)$  explicitly gives correct results, but computation is reduced by searching in  $\phi$  and  $\lambda$  only, and adjusting  $T_0$  within each iteration to make the mean (over  $r$ ) value of  $(\Delta T(s, r) - O(r))/\sigma^*(r)$  zero.

The expectation value for  $\chi^2$  after minimisation is given by the total number of DOF remaining:

$$\hat{\chi}_{min}^2 = -K + \sum_{s=1}^S (R(s) - 3) \quad (4)$$

$$K = 0 \quad \text{if } O(r) \text{ are prior values} \\ = R_{MAX} \quad \text{if } O(r) \text{ are included as DOF}$$

$$\hat{\chi}_{min}^2 = \text{Expectation value for } \chi_{min}^2$$

$$R_{MAX} = \text{Overall number of outstations used in network}$$



as there are  $R(s)$  initial DOF (observations) for each flash, of which 3 are lost estimating  $T_0$ ,  $\phi$ ,  $\lambda$ ; and one further DOF is lost overall for each of the offsets  $O(r)$  which may have to be estimated — one for every outstation used.

As before, with prior variances (and offsets) minimisation of  $\chi^2$  fixes  $S$  flashes. With many flashes,  $\chi^2$  can be scaled to its expectation value by assuming a relative relation between the components of  $\sigma^*(r)$ , and scaling its absolute value, via (4), to provide the best estimate of mean timing variance for each outstation. Note that  $\sigma^{*2}(r)$  is the variance of a single arrival time; distinct from the ATD variance  $\sigma^2(r)$  defined in (1) which depends on two timing variances, and for equal components of  $\sigma^*(r)$  is approximately a factor of two larger. (The exact relation may be complicated by the fact that one timing variance is consistently added to all the others).

If the flashes originated from a small area, and within a short period of time, then the offsets introduced into timing measurements at each outstation due to timescale errors and/or propagation effects are essentially constant. (Any variation increases  $\sigma^*(r)$ , giving a pessimistic estimate). Thus we may estimate  $O(r)$  by including these as DOF within the minimisation, together with the normal independent variables. This produces marginally modified fixes, yields estimates of the offset biases  $O(r)$ , and also estimates of the timing scatter  $\sigma^*(r)$  about these biases. Monte-Carlo methods may be used to deduce the fixing scatter from  $\sigma^*(r)$ , or alternatively calculating  $\sigma(r) = (2^{1/2})\sigma^*(r)$  allows  $\sigma(r)$  to be interpreted through diagrams such as Fig. 2.

The minimisation may be carried out by fixing flashes (independently) within an inner iteration, and adjusting  $O(r)$  in an outer iteration; double precision arithmetic is necessary to converge accurately.

#### *d. Variances and fix errors from trial case data*

In the Massif Centrale study mentioned above (Lee, 1989b), setting  $O(r)$  to zero, and  $\sigma(r)$  equal, indicated  $\sigma(r)$  of 5  $\mu$ s near the Massif Centrale, corresponding (with trial geometry) to an absolute fix error of 5 km. The ATD system fix pattern was generally supported by observer evidence and insurance damage reports, although it is difficult to trust observer evidence to better than 10–15 km. Allowing  $O(r)$  to vary (and accounting for lost DOF) reduced the (relative)  $\sigma(r)$  to 1.9  $\mu$ s, corresponding to a fix scatter (superimposed on a bias) of 1.8 km. In practice there was clear evidence that the components of  $\sigma(r)$  should not be equal. Setting their ratios to that indicated by the ATD SNR, the best estimate of absolute  $\sigma(r)$  between Beaufort Park (reference station) and Camborne Gibraltar Shanwell was 0.84, 1.72 and 1.92  $\mu$ s respectively, corresponding to a fix scatter of 0.88 km. The actual values of  $O(r)$  were similar for both ratios of  $\sigma(r)$ , and the only sizeable offset (3  $\mu$ s for the Beaufort Park to Shanwell path) corresponded roughly to the sign and magnitude expected from propagation effects alone.

The ATD system does not measure bearings, but as a comparison the scatter in back-bearing between the fixes and the outstations with this type of fix scatter is of the order of a few hundredths of a degree, comparable with the scatter in back-bearing measured for the tightest Mediterranean groups described above (Lee, 1986a).

Thus the scatter in ATD extraction superimposed on a bias that might be eliminated by adequate clocks and a knowledge of ionospheric propagation was less than 2  $\mu$ s. With just four trial outstations operating at ranges of around 1000 km, this translated into a fix scatter of 0.9–1.9 km.

## 5 Case studies from the pre-operational ATD system

### *a. Background*

This Section presents two cases using data from the pre-operational UK Meteorological Office ATD system, although non-operational fixing algorithms are used. At this stage of installation only the five UK outstations were operating, limiting the system's ability to report long-range fixes reliably; epoch calibration was performed only crudely; and spectral calibration was not routinely performed. However, in spite of any systematic effects which these pre-operational short-cuts may have introduced, the data is amenable to the type of analysis performed above which eliminates bias.

### *b. Case: July 29, 1987*

This case comprises 41 UK-area flashes detected between 1500–1511 GMT (Greenwich Mean Time). Shortly prior to this period a NAVSTAR receiver had established epoch calibration at each outstation,



which was subsequently maintained via Loran-C reception.

Fig. 3 is re-drawn from a routine FRONTIERS (Lee and Collier, 1985) rain-radar map of south-east UK for 1455–1500 GMT, and shows rain-bands aligned along the Suffolk-Essex coastline, with 5 by 5 km rainfall peaking above  $64 \text{ mm h}^{-1}$ ; the most active regions were moving slowly ESE. ATD fixes for 1500–1505 GMT are superimposed on expanded regions showing their approximate correspondence with the heaviest rainfall areas. This crude comparison is limited by the five-minute discrepancy in time and coarse spatial resolution of the radar data, and because the systems observe different quantities; but does at least indicate a lack of gross location errors from unknown sources. As systematic errors may exist no detailed comparison with rain-radar data is made.

Throughout, activity was close to Hemsby; data was often unavailable there, presumably because gross equipment overload prevented data reporting. Occasionally sferics were unavailable at other outstations, so flashes were located using five- or four-sferic data, using the techniques of (2)–(4). Offsets  $O(r)$  were initially set to zero to estimate absolute errors. Of 41 fixable flashes two were rejected as their  $\sigma(r)$  values (1) were 71 and 72  $\mu\text{s}$  respectively, well outside the 40  $\mu\text{s}$  quality limit (Lee, 1986a), implying peak mis-match during correlation caused by waveform distortion. The remaining 39 flashes gave  $\sigma^*(r)$  4.6  $\mu\text{s}$  (equivalent  $\sigma(r)$  6.5  $\mu\text{s}$ ) based on 51 DOF — enough to give a good estimate. Monte-Carlo simulation using the five outstation locations and 4.6  $\mu\text{s}$   $\sigma^*(r)$  estimated 3 km fix error in this region; loss of Hemsby roughly doubles the error. Had all seven operational outstation sites been available with  $\sigma(r)$  of 6.5  $\mu\text{s}$ , Fig. 2 indicates that fix errors would have been much smaller.

Calculation of relative errors, allowing  $\chi^2$  minimisation to include  $O(r)$ , reduces the DOF by the four non-reference outstations to 47; and reduces  $\sigma^*(r)$  to 1.1  $\mu\text{s}$ . The resulting  $O(r)$  relative to Beaufort Park reference (ie. offsets to ATD rather than the smaller timing offsets whose sum would be zero) are listed in Table 1. The absolute values are not necessarily meaningful given the potential for calibration errors, but were clearly enough to degrade  $\sigma(r)$  substantially. The timing scatter is now more accurately represented by a Gaussian distribution with variance  $\sigma^*(r)$  (as bias has been eliminated) and a Monte-Carlo exercise equates this to 700 m RMS scatter in (relative) five-station fixing in this area.

On this occasion, after fitting  $O(r)$  it was not judged necessary to reject further flashes on the basis of their individual variance being significantly different from those of a standard  $\chi^2$  distribution containing all the other flashes — an effect associated with slight amplitude overloading (Lee, 1989b). However, one flash was close to the 0.1% significance level set as a rejection threshold (Lee, 1989b), and elimination of this would have reduced  $\sigma^*(r)$  slightly to 1.0  $\mu\text{s}$ .

Although the amount of data in this case is small, conclusions can be drawn:

- i. The absolute ATD error  $\sigma(r)$  of 6.5  $\mu\text{s}$  exceeds the best estimate (3.3  $\mu\text{s}$ ) from the sferics trial (Lee, 1986a). Nevertheless, even when using only UK outstations a useful 3–6 km absolute location error was achieved, allowing comparison with the 2–5 km UK weather radar resolution.
- ii. More significantly, a relative timing error  $\sigma^*(r)$  of 1.1  $\mu\text{s}$  ( $\sigma(r)$  of 1.6  $\mu\text{s}$ ) was measured. This suggests that the data compression techniques incorporated into the operational ATD system do not degrade timing to the extent feared by Lee (1986b).
- iii. For the UK location region considered, the low  $\sigma^*(r)$  values imply five-station fixing with 700 m relative location error.
- iv. There is considerable scope for reduction of bias errors so that absolute location errors can approach the relative value indicated above.

### c. Case: September 5, 1987

Thirty-eight days later with the same outstations, 274 flashes were fixed between 1430–1900 GMT within a similar geographical area (shaded in Fig. 4), with heaviest flash rates moving roughly SE.

Of these, 29 flashes were immediately rejected as their individual  $\sigma(r)$  values exceeded 40  $\mu\text{s}$  (most exceeded 70  $\mu\text{s}$ ). While fitting  $O(r)$ , 13 more flashes were excluded because their  $\sigma^*(r)$  exceeded a 0.1% significance threshold, discussed above. This left 232 acceptable five- or four-station flashes, contributing 365 DOF to a 0.95  $\mu\text{s}$  estimate of relative  $\sigma^*(r)$  (equivalent  $\sigma(r)$  1.34  $\mu\text{s}$ ), corresponding to a relative flash location error of 630 m after bias removal. Thus the earlier result, based on much less data, is supported.

The fitted  $O(r)$  values for the entire period (Beaufort Park subtracted), are also listed in Table 1, and differ from the earlier operational case. As  $\sigma(r)$  estimates residuals remaining after differencing



Station	Absolute Offset Values ( $\mu s$ )		
	July 29	Sept 5	Difference
Hemsby	-6.6	14.2	20.8
Camborne	-7.2	23.1	30.3
Stornoway	-2.2	7.0	9.2
Lerwick	1.8	13.3	11.5
Beaufort P.	0.0	0.0	0.0

Table 1: Fitted Offsets  $O(r)$ ,  $\mu s$

quantities which include  $O(r)$ , as well as individual flash variation and system noise effects, this implies the offsets remained constant to at least this level over the entire period and over the entire area.

The offsets  $O(r)$  were fitted for sub-intervals of 30 minutes from 1430–1700, and 60 minutes from 1700–1900 GMT when activity was declining. Results in Fig. 5 present  $O(r)$  with respect to Beaufort Park as reference (ie. as ATD offsets); and sunset time at the ground if atmospheric refraction is ignored (Smithsonian, 1951), after which propagation variations are expected (Watt, 1967). Mean  $O(r)$  are shown as dashed lines. Time variations in  $O(r)$  are roughly consistent with  $\sigma(r)$  of 1.34  $\mu s$  if it is assumed that  $O(r)$  varies on a time scale comparable with 30 mins.

The small value of  $\sigma(r)$  and associated relative constancy of  $O(r)$  over several hours makes propagation an unlikely reason for the discrepancy in  $O(r)$  between the two similar cases presented here. However, when  $O(r)$  differences (Table 1) are taken modulo 10  $\mu s$ , the mean of their values is 0.5  $\mu s$  with a standard deviation of 1  $\mu s$  (comparable with  $\sigma(r)$ ). Outstations were stopped and re-started several times between the two dates, and it would appear that in attempting to re-establish epoch using only Loran-C the operators locked onto incorrect zero-crossings spaced by multiples of 10  $\mu s$ , inadvertently re-basing timescales! Clearly, this is a potential problem for any system using Loran-C for epoch maintenance. Apart from this problem of detail (addressed in Appendix A), the offsets are consistent between the two cases presented.

## 6 Case studies from the operational ATD system

### a. Background

Outstations were later established at Gibraltar and Cyprus; but for administrative reasons unconnected with fundamental ATD system operation their overseas communications links initially proved unreliable, and few early data including overseas outstations have been studied. Nevertheless, these data are sufficient to identify loose groups of flashes, and analyse them as above. The longer base-lines allow relative accuracy studies at greater ranges where the impact of earth-ionosphere waveguide propagation is important.

### b. Case: December 4, 1987

VLF propagation is most consistent near mid-day when the ionospheric D-Layer height is stable. Thus data were sought with sferics available from most outstations, occurring broadly within the local ‘midday period’ throughout the propagation path, and for which loose clusters of fixes were observed. On December 4 1987 from 1000–1200 GMT three such clusters from different areas were observed and separately analysed using relations (2)–(4). Table 2 presents results, with cluster position means and standard deviations (spread) indicating the regions assumed to provide ‘similar’ offsets. The number of flashes in each cluster is given, the number of DOF they contribute to estimating relative  $\sigma^*(r)$ , and relative  $\sigma^*(r)$  itself. The relative flash location error (fix scatter) was estimated from  $\sigma^*(r)$  by a Monte-Carlo technique for appropriate 7- or 6-outstation geometry, and is also shown.

The only cluster (A) within the normal service area fixed off the west coast of Portugal, in a difficult area for fixing (Fig. 2), in the vicinity of a depression and associated frontal lines. Cluster B fixed west of the service area, some 1200 km east of Atlantic City USA, in fair agreement with an analysed frontal



Cluster	Centre		Spread		Flashes	DOF	$\sigma^*(r)$ ( $\mu s$ )	Fix Error (RMS km)
A	38.3N	11.6W	0.6N	1.7E	34	88	1.35	1.3
B	40.3N	61.1W	1.0N	2.8E	48	140	1.24	7.3 (6-station)
C	8.2N	21.1W	0.8N	1.8E	48	170	1.27	7.3

Table 2: Location of Clusters, and their Scatter, Dec 4 1987

Cluster	Hemsby	Camborne	Stornaway	Lerwick	Cyprus	Gibraltar	Beaufort P.
A	3.8	-4.5	-10.4	4.0	-5.8	-1.4	0.0
B	5.9	-4.7	-2.3	0.6	—	0.2	0.0
C	4.8	-7.5	-13.2	0.9	-3.9	-12.3	0.0

Table 3: Dec 4 1987: Offsets ( $\mu s$ ) Necessary to minimise  $\sigma^*(r)$

trough. Cluster C fixed south of the service area, approximately 1000 km west of Sierra Leone, in a position agreeing with Meteosat cloud imagery. Broad agreement in flash location was thus obtained with other techniques; but this depends on errors of epoch and spectral calibration, and propagation effects. We concentrate here on the scatter that remains when such effects have been eliminated.

Despite these clusters' different locations, Table 2 shows that once offsets have been removed  $\sigma^*(r)$  is around 1.3  $\mu s$  (equivalent  $\sigma(r)$  1.8  $\mu s$ ), only slightly larger than the values obtained for the UK-only outstations with UK flashes. Fix scatter is correspondingly small in spite of the extreme ranges involved.

Table 3 shows the offsets (relative to Beaufort Park) fitted to obtain Table 2: cluster B has no Cyprus entry as few sferics were received. Absolute values are unimportant; but because the data gathering periods were short and overlapping, offset differences between clusters (especially at Gibraltar and Stornaway) are significant as they substantially exceed the scatter within a cluster.

Offset variation with flash position occurs because the phase velocity of 1.004c (c is free-space light velocity) deduced from trials data (Lee, 1986a) is a poor fit to waveguide phase velocity over all paths. At sufficiently large ranges VLF propagation is dominated by the first order waveguide mode, as higher modes are heavily attenuated (Watt, 1967). Fig. 6, after Wait and Spies (1965), shows first mode north-south phase velocity variation with frequency, for a model daytime ionosphere and various surface conductivities. At frequencies near 9.8 kHz the 1.0054c velocity for 'infinitely' conducting surfaces (essentially sea-water) reduces through 1.0050c and 1.0038c for conductivities of 10 and 1 millimho  $m^{-1}$  (rich damp soils to dry sandy soils respectively), to 1.002c–1.000c for low conductivity of 0.2–0.06 millimho  $m^{-1}$  (exceptionally arid or freshwater/ice regions). Velocity variations up to  $\pm 0.0005c$  (near 10 kHz) occur with bearing — the greatest effect being a reduction in velocity for East- and especially West-propagating waves near the geomagnetic equator (Swanson, 1968: unpublished). Furthermore, the effective phase velocity is modified by variations in ionospheric profile, by the observed spectra (determined by source and path-attenuation spectra as well as the instrument spectral profile), and the contaminating presence of faster higher-order modes at shorter ranges.

The three clusters were composited by allowing for geographical velocity variation. One set of offsets was assigned to the composite cluster, and relations (2)–(4) were iterated (minimising  $\chi^2$  by adjusting offsets and flash positions) while simultaneously adjusting sferic phase velocities within  $T_{TH}$ . Clusters A and B were each assigned a single (iterated) velocity, as from each cluster the propagation paths to all outstations were roughly similar. Morgan's (1968) conductivity map indicates broadly similar ground paths from cluster C, off Sierra Leone, to UK and Gibraltar outstations; but the Cyprus path over the Sahara desert has substantially lower conductivity, so two (iterated) velocities were assumed for two classes of path.

The unconstrained minimisation fitted sferic phase velocities of 1.0043c for cluster A (approximating



Cluster	Duration (GMT)	Centre		Spread		Flashes	DOF	$\sigma^*(r)$ ( $\mu s$ )
All	1900–2230	—		—		49	157	8.4
D	1952–2044	10.8N	44.7W	0.6N	0.8W	7	21	0.9
E	2129–2214	11.1N	39.4W	0.3N	1.6W	4	5	1.4
F	1906–2045	11.0N	76.5W	0.4N	2.8W	7	18	4.3
G	2051–2214	11.5N	74.4W	0.6N	0.8W	12	32	1.3
H	1909–2227	14.4N	79.0W	0.6N	0.9W	17	46	1.4

Table 4: Location of Clusters, and their Scatter, Dec 3 1987

Cluster	Hemsby	Camborne	Stornaway	Lerwick	Cyprus	Gibraltar	Beaufort P.
D	4.6	-3.3	11.7	24.8	-1.5	38.1	0.0
E	4.8	-3.0	-7.1	8.2	—	1.0	0.0
F	5.7	-6.3	-3.8	6.4	7.1	1.3	0.0
G	5.5	-5.7	-7.6	2.8	-2.7	0.3	0.0
H	7.1	-7.1	-2.9	6.1	20.9	-3.4	0.0

Table 5: Dec 3 1987: Offsets ( $\mu s$ ) Necessary to minimise  $\sigma^*(r)$

the trial estimate within the normal service area); and 1.0026c for cluster B. The latter value is low for 9.8 kHz sea-paths, even for easterly propagation. However, the spectral peak frequency for observed sferics increases slightly with propagation distance; and for 5000 km range peaks near 11 kHz (Wahedra and Tantry, 1966), where Fig. 6 shows lower velocities are appropriate. For cluster C consistent velocities of 1.0025c were fitted over the paths to UK and Gibraltar, and 0.9966c over the Saharan path to Cyprus.

The minimum  $\sigma^*(r)$  for the composite data set, corresponding to these velocities, was 2.33  $\mu s$ . Its significant excess over values for individual clusters (Table 2) demonstrates the simplistic propagation model's inadequacy. However, Fig. 2 maps this into a satisfactorily small fix error, showing that even crude propagation concepts (easily updated from operational data) are usefully applicable to large areas during mid-day periods.

### c. Case: December 3, 1987

A contrasting long-range example occurred the previous evening, when 49 flashes were observed in the far south-west (approximately 10–15N and 38–80W) between 1900–2230 GMT, during twilight and night over the path.

Initially all data were grouped: after offset removal (standard 1.004c phase velocity)  $\sigma^*(r)$  was high at 8.4  $\mu s$ . However, individual ( $ATD_{TH} - ATD_M$ ) discrepancies indicated natural clustering by flash location and epoch; and as most outstations contributed to each fix, enough DOF were available to estimate  $\sigma^*(r)$  for each cluster (Table 4, D–H). Values of 0.9–1.4  $\mu s$  were found, except for cluster F (4.3  $\mu s$ ).

The large  $\sigma^{*2}(r)$  for composite data is consistent with the offset variation between clusters at each outstation caused by changing ionospheric tilt during twilight, which produces phase shifts of tens of microseconds (Watt, 1967), although this is reduced for differences between stations (Table 5). Provided tight time/space groupings of flashes are made, and rapid ionospheric variations such as those of cluster F can be avoided, it appears possible to maintain low  $\sigma^{*2}(r)$  comparable with daytime values, although phase shifts through twilight are less amenable to simple modelling than daytime phase.



## 7 Discussion

The VLF ATD system achieves high timing precision because flashes are imaged as points. Propagation ducting at VLF ensures spheric detection at megametre ranges; the combination gives accurate long-range fixing. Accuracy is enhanced as errors are statistically reduced by data from many long-range outstations; and fix over-determination allows effective quality control.

Fixing errors depend on ATD errors ( $\sigma(r)$ ). Trial and operational system results have shown that even without bias removal  $\sigma(r)$  values of 3–5  $\mu\text{s}$  have been achieved, although actual values vary with systematic errors of calibration and propagation modelling. With the operational network, 3–5  $\mu\text{s}$  values indicate (Fig. 2) absolute fix errors of around 900 m within the UK, and 1–5 km over most of Europe.

For 'clusters' of fixes from small areas and short time duration correctable bias errors are constant, and can be analysed away, leaving the scatter that correction cannot reduce. Analysis of trial and operational system data for flashes within the UK, the normal service area, and at extreme ranges (both for mid-day and for twilight periods) indicates a residual ATD scatter of about 1.4–2.0  $\mu\text{s}$  except during rapid twilight phase variability.

Watt (1967, section 3.5.5) discusses short-term random phase perturbations to received 10 kHz transmissions: by day the RMS phase deviation (in time units) increases from 1.0–1.7  $\mu\text{s}$  as range increases from 1–10 Mm, and is a factor 2.4 larger at night. At 1–6 Mm range the correlation coefficient between phase fluctuations at receivers 200 km apart is a few tenths, so ATD fluctuations between phases received over two paths (ie.  $\sigma(r)$ ) is further enhanced by a factor 1.4. Thus experimental ATD scatter values broadly agree with Watt's observations, lending credence to their values, and suggesting that system details have not degraded ATD noise.

These low (1.7  $\mu\text{s}$ )  $\sigma(r)$  values correspond (Fig. 2) to fix scatter (after bias removal) of around 1.2 km over most of Central Europe for the operational seven-outstation network.

Thus fixing patterns and absolute locations are potentially observable with great precision. Lee (1989b, section 8) describes observations (by five outstations at 1000 km range) of apparent motion of an organised storm over a 3 km path along the hodograph vector direction, as expected for an R-moving storm cell (Wilhelmson and Klemp, 1981). Absolute  $\sigma(r)$  values only a factor of two larger than the relative values described above have been demonstrated on occasion, suggesting that with care bias elimination has been approached. Furthermore, the ATD technique design has deliberately emphasised stringent quality controls during ATD extraction and fixing to minimise the rate of 'bad' fixes well outside the normal error distribution.

Basic equipment epoch resolution is around 0.1  $\mu\text{s}$ . Spectral calibration/correction techniques monitor equipment filter profiles to detect catastrophic failure, and also to correct for minor deficiencies due to component tolerance or aging — including long-term corrections to filter group delay at this level of precision.

Appendix A discusses the techniques available for epoch calibration and maintenance, and shows that epoch can be held to a negligible error of around 0.2  $\mu\text{s}$ .

Appendix B discusses a hierarchy of possible techniques for propagation bias elimination. The simplest monitors mean offsets as described above (incorporating external data where available), and applies them as a correction. More sophisticated approaches use a VLF propagation model to reduce offset. In this study daytime long-range spheric velocity variation was crudely parameterised, reducing ATD deviation to within a factor 1.8 of its irreducible value, so simple models can provide useful benefits. Multi-frequency (spectral) models can correct sferics for differential propagation distortion, improving SNR, and dramatically reducing the probability of ATD extraction one or more VLF cycles in error (a cause of data loss through subsequent flash rejection). Finally, the model itself can be slowly refined using residual differences between associated spheric waveforms. Sudden ionospheric disturbances remain as a temporary (but identifiable) problem for periods of around an hour.

Reduction of ATD bias, and perhaps of normally distributed scatter, would improve flash location. Perhaps more important, the associated tightening of data self-consistency would strengthen early discrimination against internal errors. In the cases described, several flash  $\sigma(r)$  exceeded 40  $\mu\text{s}$ , leading to flash rejection because an ATD value was probably extracted whole VLF cycles in error (cycle slipping). Once 'acceptable'  $\sigma(r)$  values are not inflated substantially beyond 2  $\mu\text{s}$  by bias errors, it becomes easier to identify ATD values in error by 100  $\mu\text{s}$ , and so to re-examine the fix consistency of alternative ATD correlogram peaks. The task becomes more reliable if cycle slipping is rare enough never to occur on more than one spheric within a flash — the likely situation with spectral propagation



models. Thus ATD extraction becomes more robust, so that less data is lost through quality control, as well as more accurate.

When flashes are fixed with unfavourable fixing geometry (usually at long range when some outstations are unavailable) the  $RESIDUAL^2(\phi, \lambda)$  surface (1) may exhibit local minima away from the global fix position, to be found by the iterative (searching) fix algorithm. Small values of  $\sigma^2(r)$  raise the surface height outside the global minimum, improving the search-driving slope towards it; and also distinguish the local value from that expected, so the searcher is alerted and looks elsewhere. The combination of higher ATD precision and improved robustness against local minima means that operations can be maintained over wide service areas even when some outstations may be unavailable for technical reasons. The reduced data loss described in the previous paragraph is also important under these conditions.

## 8 Conclusions

With VLF observation, lightning flashes appear as point images, with dimensions well below 100 m. This consistent appearance allows precise flash location, even at megametre ranges, if bias effects can be removed.

A case study of daytime UK-received sferics, whose flashes fixed in the south-eastern UK, showed apparent biases to theoretical sferic transit times that were consistent over several hours, and between situations 38 days apart. Removal of this bias left ATD scatter at around  $1.4 \mu\text{s}$ . (Such bias corrections are not made in the current operational system). For the observed region, using the five UK outstations only, this time-difference scatter corresponds to 650 m location error.

Other short-period and limited area cases were studied, covering overseas outstations and flashes at much greater ranges, under daytime, twilight, and night conditions. Bias elimination gave broadly similar normal ATD distributions of deviation  $1.4\text{--}2.0 \mu\text{s}$ , provided rapidly-changing twilight situations are avoided. Other workers using long-range VLF reception for navigation purposes have observed similar levels of phase-difference variation. With successful bias correction, and all seven operational ATD outstations contributing to fixing with this ATD error, flashes would be fixed over most of western Europe with 1.2 km error.

It is shown that poor epoch calibration can be a major source of bias; but is entirely avoidable. With correct procedures, spectral calibration bias is also negligible.

The remaining source of bias is VLF propagation. The case studies, and Omega navigation experience, indicate that bias can be corrected to approximately the scatter levels discussed above. Suitable propagation models exist, and techniques are discussed for refining these models into agreement with measured sferics. Difficulties remain during sudden ionospheric disturbances, but these are limited to an hour or so, and are readily detected.

The potential benefits of the above improvements in technique lie in the increased accuracy and robustness of an operational system, which should alleviate degradation in wide-area coverage in the face of any temporary outstation loss.

*Acknowledgements* I am indebted to Mr D Jerrett and his staff for the ATD data for this study, and to Mr R Brown and his staff for FRONTIERS data.

## Appendix A Elimination of Epoch Calibration Bias

It has been demonstrated that epoch calibration errors can substantially exceed uncorrectable timing scatter. To eliminate this, calibration at each site must be established (by travelling atomic clock, or NAVSTAR techniques: capable of errors under  $0.2 \mu\text{s}$ ) and maintained. The prime operational maintenance technique is Loran-C reception: resolution around  $0.1 \mu\text{s}$ . However Loran-C's  $10 \mu\text{s}$  cycle ambiguity can cause problems after equipment failure, so Omega VLF techniques are also implemented operationally. The  $1\text{--}2 \mu\text{s}$  stability of mid-day Omega reception at 10.2 kHz resolves Loran-C ambiguity, so Loran-C and 10.2 kHz Omega together extend ambiguity to  $98 \mu\text{s}$ . Reception of a second Omega



frequency at 13.6 kHz extends ambiguity to the reciprocal of the Omega difference frequency, or 294  $\mu$ s, enough to allow further ambiguity to be resolved through low frequency (LF) modulated time-clock transmissions.

Ambiguity resolution depends on timing recognised features in waveforms whose appearance and phase may be site dependent. However, if timed records of waveforms (and features) are made soon after establishing epoch, and at intervals thereafter (allowing diurnal/seasonal tracking), this aids the recognition process making it reliable.

In addition, this paper's case studies have demonstrated that under suitable conditions of outstation/flash location geometry 'offsets' in epoch can be estimated from lightning data to sufficient precision to resolve Loran-C ambiguity directly. Alternatively, NAVSTAR receivers could be installed.

Thus maintenance of epoch to an insignificantly small error of around 0.2  $\mu$ s need not be a problem.

## Appendix B

### Elimination of Propagation Bias

Once epoch errors are eliminated there remain propagation biases, with a hierarchy of possible alleviation techniques.

The simplest technique determines the offsets for each receiver outstation, as a function of flash location (and diurnal/seasonal cycle), necessary to reduce bias. The technique is applied with little extra computational cost by approximate fixing, applying appropriate offsets, then continuing the final (rapid) stages of iterative fixing into the perturbed minimum.

Offset estimation is achieved by averaging many flashes as described in the main text; and/or correcting fixes with more precise external data. An important special case occurs where some flashes are fixed using all outstations, minimising fix errors; thus reducing offset (and fix) errors when some outstations become unavailable. The task is eased when offsets vary only slightly over a wide area, as demonstrated by the case studies above.

Propagation imposes a spectral transfer function on the sferic source waveform, so timing offsets are not strictly constant with flash location but depend on the source waveform. The function is conveniently expressed as a slowly-varying correction spectrum to a nominal constant pure-real phase-velocity. After initial fixing the propagation spectrum for each flash-outstation path is roughly calculable using a theoretical model. Thus, in a more sophisticated bias elimination technique, for each ATD path-pair the two received sferic waveforms are spectrally corrected to an arbitrary path intermediate to the actual paths travelled, to reduce the differential distortion imposed by the different paths on the original source waveform. This spectral correction is applied at low computational cost as the sferic's Discrete Fourier Transform is already available from the earlier ATD extraction process; and is limited in time duration to the known vicinity of the correlation peak (Lee, 1986a; end of Appendix C) reducing computation for the final Transform in ATD re-extraction. Finally, fix iteration from the initial fix is continued as before. This enhancement to  $ATD_{TH}(r)$  in the algorithms used in the case studies offers several advantages: (a) Regarding theoretical propagation models as first estimates to be (robustly) refined by offsets as described above implies they can be simple, and represented by a small number of disposable parameters. Nevertheless, the geographical regions that can be associated with an estimated offset value will be extended, reducing the necessary storage for offset estimates, and making more flash data available for each offset estimation. (b) Reducing differential propagation effects (making sferics more similar) before ATD extraction through correlation has a dual advantage. When the waveforms are correctly matched in time (in the appropriate ATD lag position), the correlation peak is higher, increasing SNR (Lee, 1986a; Appendix C), to reduce normally distributed ATD error. Additionally, relative to this enhanced main peak, the SNR for subsidiary peaks (lags slipped by whole cycles) is reduced, dramatically reducing the probability of estimating ATD in error because of distorting propagation effects.

Information for suitable propagation models is widely available. Wait and Spies (1965) give curves for phase velocity (eg. Fig. 6) as well as attenuation and mode excitation factors for various waveguide modes. Morgan's (1968) VLF ground conductivity map allows geographical effects to be included. For the special Omega navigation system frequencies, with sources at Omega transmitters, a wealth of experimental data has been used to refine the theoretical prediction of VLF received phase (Swanson, 1976; Morris, 1978; Gupta and Morris, 1986).



Finally, internal information from the ATD system itself can be used to refine model spectra so that unbiased waveform matching is eventually achieved. This could be done essentially by taking the quotient of the nominally corrected sferic spectra in an ATD-extraction pair, and regarding this as an 'error signal' to evolve best estimates of the model spectra for a single region (and portion of the diurnal/seasonal cycle), using Kalman-filter techniques. This is likely to be most successful if the initial prior model is well founded theoretically.

The above text relates to normal geographical and diurnal/seasonal variations. There can occur sudden ionospheric disturbances, caused by (daytime) solar flares (Watt, 1967; section 3.5.5) which disturb the ionospheric phase height. These cause sudden phase anomalies which peak in a few minutes to a few tens of microseconds, then decay over a few hours — although substantial recovery is complete within one hour. These should be obvious from Omega traces and from degradation in data consistency — and an element of correction may be possible from this data, especially in the recovery phase.

## REFERENCES

- Bent, R.B., and W.A. Lyons, 1984: Theoretical evaluations and initial operational experiences of LPATS (lightning position and tracking system) to monitor lightning ground strikes using a time-of-arrival (TOA) technique, *Seventh Int. Conf. on Atmospheric Electricity*, June 3-8, Albany, N.Y., Amer. Meteor. Soc., 317-324.
- Cantor, G.N., 1967: Some observations on the polarisation spectrum of VLF radio waves, *IEE Conf. on M.F., L.F. and V.L.F. Radio Propagation*, Savoy Place, London, 8-10 Nov., Conf. Pub. 36, 246-251.
- Gupta, R.R., and P.B. Morris, 1986: Overview of OMEGA signal coverage, *Navigation*, 33, 223-249.
- Herrman, B.D., M.A. Uman, R.D. Brantley, and E.P. Krider, 1976: Test of the principle of operation of a wideband magnetic direction finder for lightning return strokes, *J. Appl. Meteor.*, 15, 402-405.
- Horner, F., 1954: The accuracy of the location of sources of atmospherics by radio direction-finding, *Proc. Inst. Elect. Eng.*, 101, Part III, 383-390.
- Krider, E.P., R.C. Noggle, and M.A. Uman, 1976: A gated wideband magnetic direction finder for lightning return strokes, *J. Appl. Meteor.*, 15, 301-306.
- Lee, A.C.L., and C.G. Collier, 1985: The detection and forecasting of lightning, *Second Int. Conf. on The Aviation Weather System*, June 19-21, Montreal, 168-171.
- Lee, A.C.L., 1986a: An experimental study of the remote location of lightning flashes using a VLF arrival time difference technique, *Quart. J. Roy. Meteor. Soc.*, 112, 203-229.
- Lee, A.C.L., 1986b: An operational system for the remote location of lightning flashes using a VLF arrival time difference technique, *J. Atmos. and Ocean. Tech.*, 3, 630-642.
- Lee, A.C.L., 1989a: The limiting accuracy of long wavelength lightning flash location, *J. Atmos. and Ocean. Tech.*, 6, 43-49.
- Lee, A.C.L., 1989b: Ground truth confirmation and theoretical limits of an experimental VLF arrival time difference lightning flash locating system, *Quart. J. Roy. Meteor. Soc.*, 115, 1147-1166.
- Lyons, W.A., R.B. Bent, and W.H. Highlands, 1985: Operational uses of data from several lightning position and tracking systems (LPATS), *Tenth Int. Aerospace and Ground Conf. on Lightning and Static Electricity*, Paris, June 10-13, A.A.A.F., 347-356.
- MacGorman, D.R., and W.D. Rust, 1988: An evaluation of the LLP and LPATS lightning ground strike mapping systems, *1988 Int. Aerospace and Ground Conf. on Lightning and Static Electricity*, 19-22 April, Oklahoma City, National Oceanic and Atmospheric Administration, (Addendum) 235-240.
- Maidens, A.L., 1953: Methods of synchronising the observations of a 'sferics' network, *Meteor. Mag.*, 82, 267-270.
- Morgan, R.R., 1968: World-wide VLF effective-conductivity map, Westinghouse Electric Corporation, Under contract N00014-67-C-0274 to Office of Naval Research, Dept. Navy, Washington DC.
- Morris, P.B., 1978: The determination of regional Omega signal characteristics through pre-



- diction, validation and calibration, *Proc. Third Annual Meeting, International Omega Association*, 26–28 Sept, London, International Omega Association Inc, PO Box 2324, Arlington, VA 22202, USA.
- Ockenden, C.V., 1947: Sferics, *Meteor. Mag.*, 76, 78–84.
- Proctor, D.E., 1983: Lightning and precipitation in a small multicellular thunderstorm, *J. Geophys. Res.*, 88, 5421–5440.
- Scott, L., 1988: A lightning location system for the UK electricity supply industry, *Int. Aerospace and Ground Conf. on Lightning and Static Electricity*, 19–22 April, Oklahoma City, National Oceanic and Atmospheric Administration, 391–395.
- Smithsonian Institution, 1951: *Smithsonian Meteorological Tables*, Washington.
- Swanson, E.R., 1968: Remarks on the propagation of 10.2 kHz electromagnetic waves: the effects of bearing, total magnetic field strength, dip angle of the magnetic field, and ground conductivity, Naval Electronics Laboratory Center, San Diego California, Tech. Note TN-1375.
- Swanson, E.R., 1976: Propagation effects on Omega, AGARD CP No. 209 on Propagation Limitations of Navigation and Positioning Systems, (Electromagnetic Wave Propagation Panel Specialists Meeting, Istanbul, 20–22 Oct 1976).
- Watt, A.D., 1967: *VLF Radio Engineering*. International Series in Electromagnetic Waves, Volume 14, Pergamon Press.
- Wait, J.R., and K.P. Spies, 1965: Influence of finite ground conductivity on the propagation of VLF radio waves, *Rad. Sci. J. Res. Nat. Bureau Standards* 69D, No 10, 1359–1373.
- Wahedra, N.S., and B.A.P. Tantry, 1966: Audio frequency spectrum of a radio atmospheric at large distances, *J. Atmos. Terr. Phys.*, 28, 1227–1232.
- Wilhelmson, R.B., and J.B. Klemp, 1981: A three-dimensional numerical simulation of splitting severe storms on 3 april 1964, *J. Atmos. Sci.*, 38, 1581–1600.
- Yamashita, M., and K. Sao, 1974a: Some considerations of the polarisation error in direction-finding of atmospherics I. Effect of the earth's magnetic field, *J. Atm. Terr. Phys.*, 36, 1623–1632.
- Yamashita, M., and K. Sao, 1974b: Some considerations of the polarisation error in direction-finding of atmospherics II. Effect of the inclined electric dipole, *J. Atm. Terr. Phys.*, 36, 1633–1641.



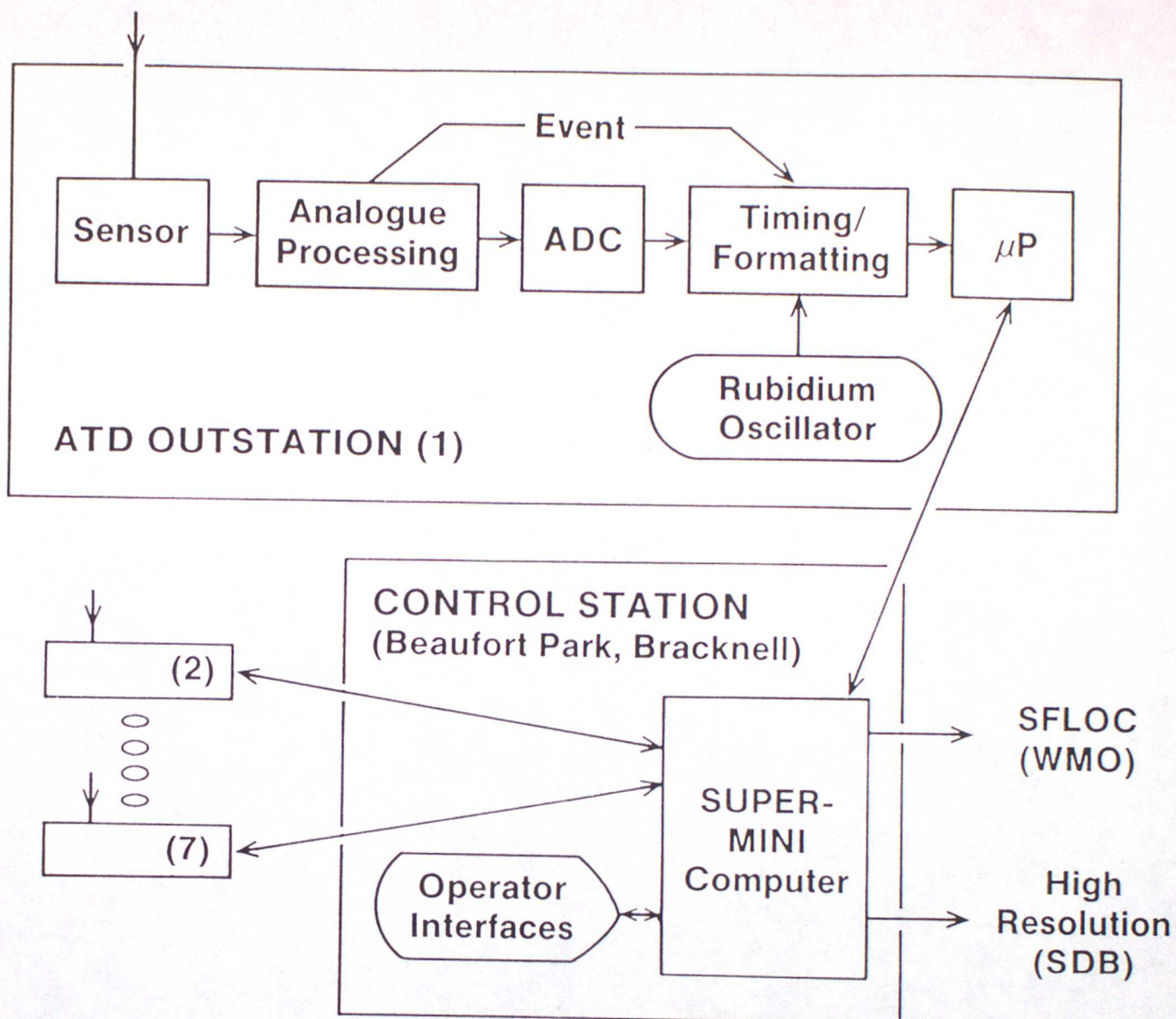


Fig. 1. Simplified representation of the seven operational ATD outstations and manned control station.



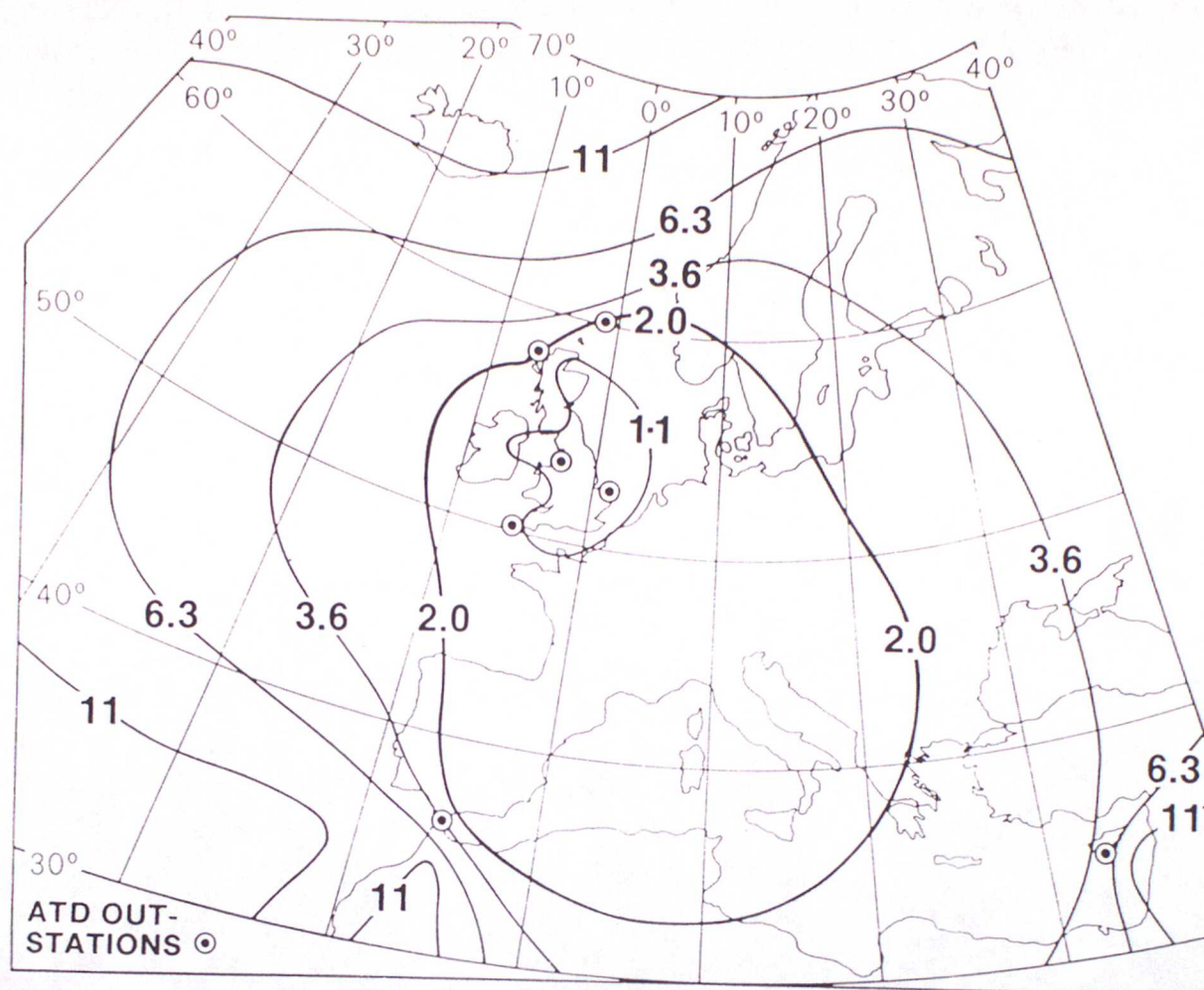


Fig. 2. Gnomonic chart showing most of the ATD system's 40W-40E 30-70N service area. Quarter-decade contours of RMS km fix accuracy, assuming  $5 \mu\text{s}$  ATD errors, are superimposed. Smaller absolute and relative ATD errors are realistic, with proportionally reduced fix errors.



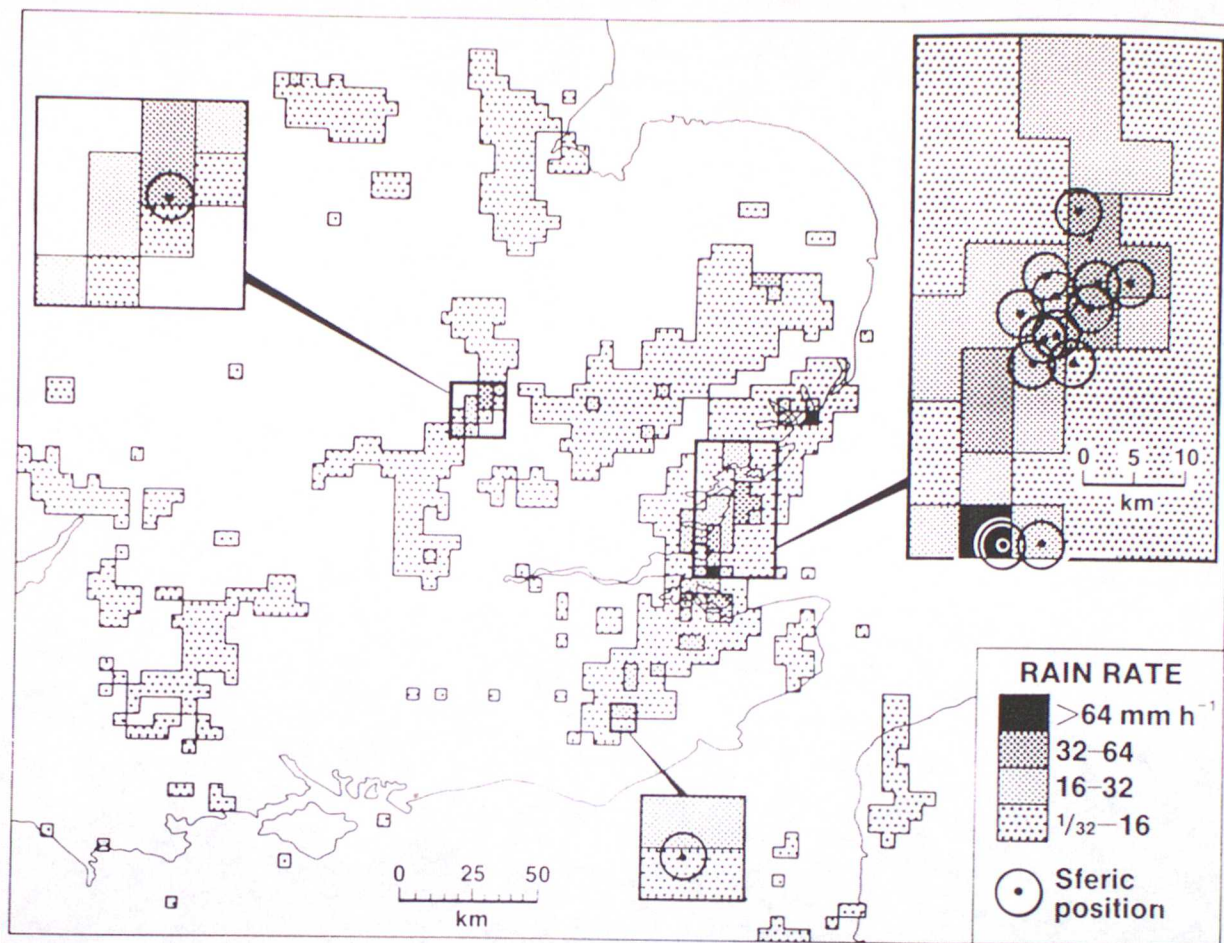


Fig. 3. FRONTIERS rain-radar data over southern UK during Case: July 29, 1987. Expanded portions have ATD sferics data superimposed to show that fixes fall close to the areas of heaviest rain. There is a 5-minute time discrepancy between ATD and radar measurements.



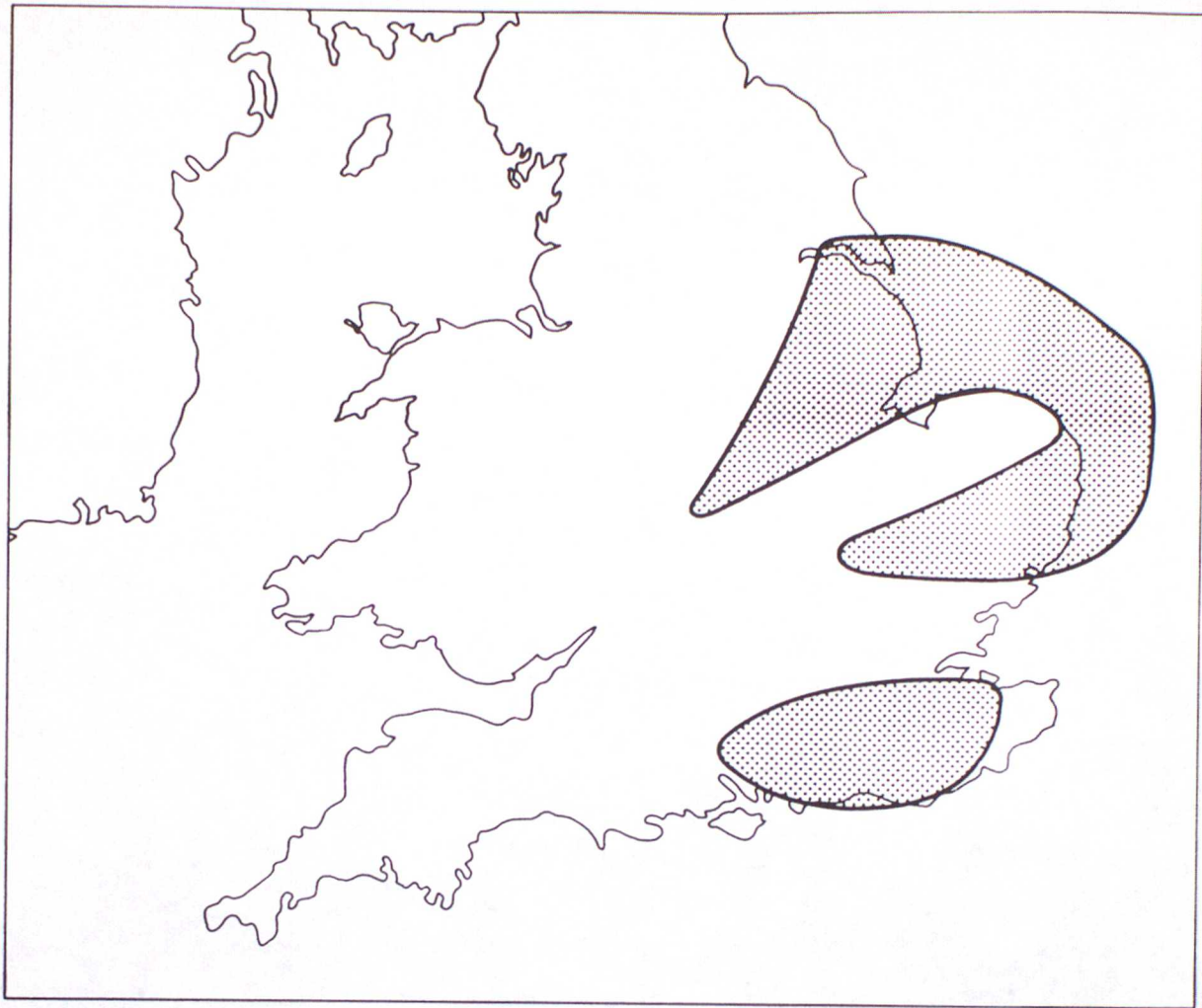


Fig. 4. The most intense lightning activity occurred over the shaded region during the 4.5 hours of Case: September 5, 1987.



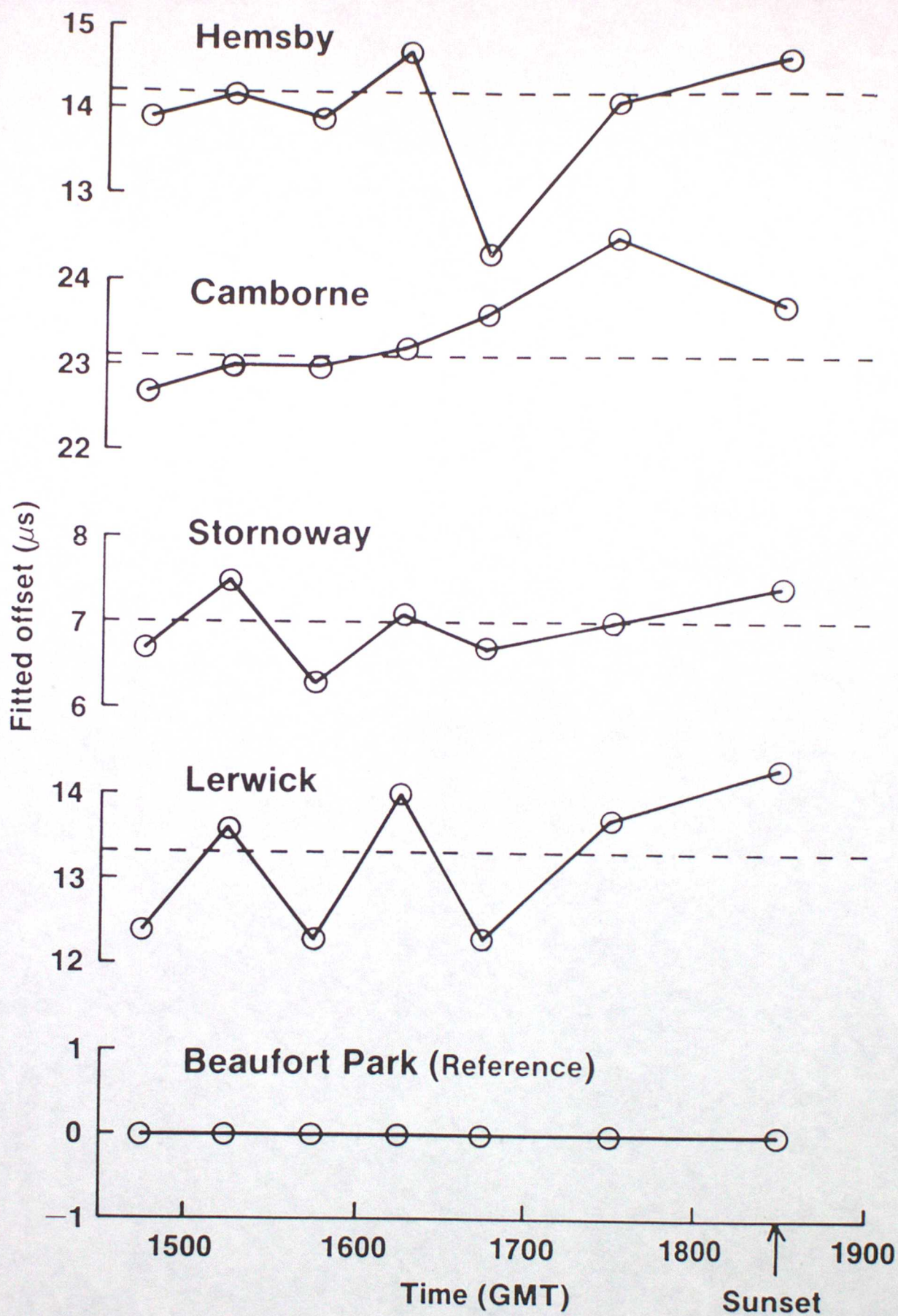


Fig. 5. Fitted (ATD) offsets that were applied to the five UK outstations to eliminate systematic bias effects, relative to that for Beaufort Park, as a function of GMT.



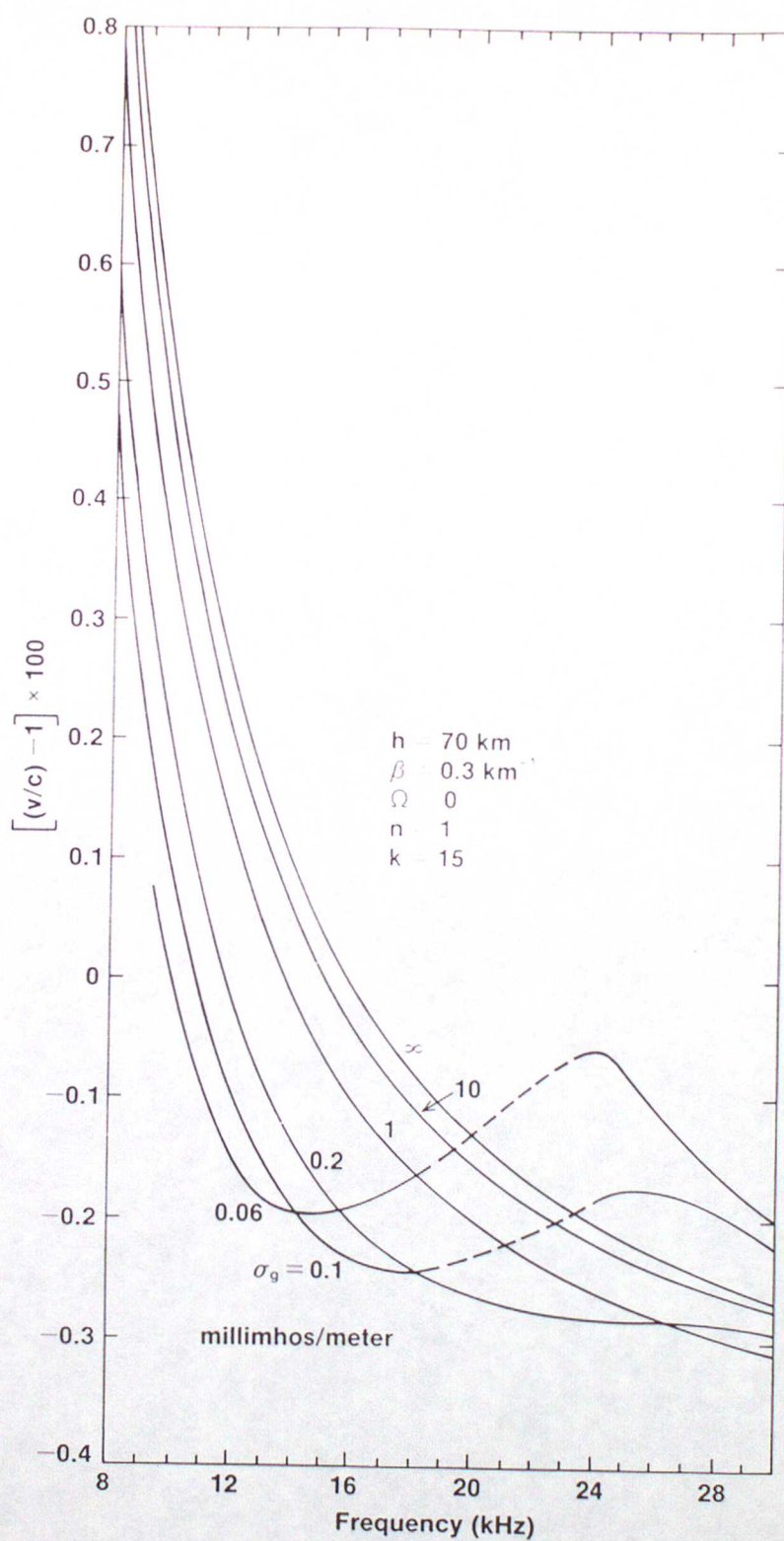


Fig. 6. Theoretical phase velocity referred to free-space light velocity  $c$  as a function of frequency, for several ground conductivities, and a daytime model ionosphere (after Wait and Spies, 1965).